

DYNAMICS OF KAONS IN NUCLEAR MATTER ^a

M.F.M. LUTZ

GSI, 64220 Darmstadt, Germany

E-mail: m.lutz@gsi.de

We consider K^- nucleon elastic and inelastic scattering in isospin symmetric nuclear matter. It is found that the proper description of the $\Lambda(1405)$ resonance structure in nuclear matter requires a self-consistent approach. Then the $\Lambda(1405)$ resonance mass remains basically unchanged, however, the resonance acquires an increased decay width as nuclear matter is compressed. The elastic and inelastic scattering amplitudes show important medium modifications close to the kaon nucleon threshold. We also construct the K^- -nuclear optical potential appropriate for K^- atoms. Our microscopic approach predicts a strong attractive non-local interaction strength.

1 Introduction

In this talk we report on recent work¹ on kaon propagation and kaon nucleon interaction in isospin symmetric nuclear matter. There has been much effort to evaluate the in medium K -mass in realistic models. Gerry Brown and Mannque Rho² suggested an effective mean field approach. Here we focus on a microscopic description of the kaon propagator in dense matter as derived from kaon nucleon scattering in free space^{3,4,5,6,7,8}.

Let us review the change of the K^+ -mass. As was emphasized in⁹ it is given by the low density theorem in terms of the empirical K^+ -nucleon scattering lengths $a_{K^+N}^{(0)} \simeq 0.02$ fm and $a_{K^+N}^{(1)} \simeq -0.32$ fm¹⁰

$$\Delta m_{K^+}^2 = -\pi \left(1 + \frac{m_K}{m_N} \right) \left(a_{K^+N}^{(I=0)} + 3 a_{K^+N}^{(I=1)} \right) \rho + \mathcal{O}(k_F^4) \quad (1)$$

where $\rho = 2 k_F^3 / (3 \pi^2)$. Model calculations^{8,6} typically find only small corrections to (1). In fact the next to leading term of order k_F^4 can be evaluated model independently in terms of the K^+N -scattering lengths

$$\Delta m_{K^+}^2 = (1) + \alpha \left(\left(a_{K^+N}^{(I=0)} \right)^2 + 3 \left(a_{K^+N}^{(I=1)} \right)^2 \right) k_F^4 + \mathcal{O}(k_F^5) \quad (2)$$

where

$$\alpha = \frac{1 - x^2 + x^2 \log(x^2)}{\pi^2 (1 - x)^2} \simeq 0.166 \quad (3)$$

^aThis talk is dedicated to Mannque Rho on the occasion of his 60th birthday

and $x = m_K/m_N$. Note that one must not expand the correction term (2) in powers of m_K/m_N . At $x = 0$ with $\alpha \simeq 0.10$ the real part of the correction term is underestimated by more than 60%.

In Fig. 1 the leading and subleading change of the K^+ -mass as a function of the Fermi momentum, k_F , is shown. The correction term is indeed small so

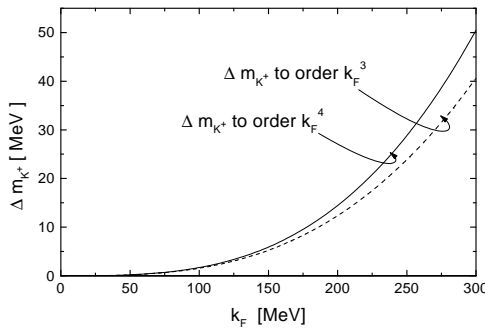


Figure 1: Change of K^+ -mass in isospin symmetric nuclear matter.

that the density expansion is useful in the K^+ -channel. At nuclear saturation density with $k_F \simeq 265$ MeV it increases the repulsive K^+ -mass shift from 28 MeV to 35 MeV by about 20%. We conclude that any microscopic model consistent with low energy K^+ -nucleon scattering data is bound to give similar results for the K^+ -propagation in nuclear matter at densities $\rho \simeq \rho_0$ sufficiently small to maintain the density expansion rapidly convergent. Consequently the role of chiral symmetry is restricted to the qualitative prediction of the K^+N -scattering lengths by the Weinberg-Tomozawa term.

We turn to the K^- -mass. At nuclear saturation the density expansion for the K^- -mode is poorly convergent if at all¹. The leading terms of the density expansion appear to contradict kaonic atom data^{12,13} which suggest sizable attraction at small density. Furthermore the empirical K^-N scattering lengths $a_{K^-N}^{(0)} \simeq (-1.70 + i 0.68)$ fm and $a_{K^-N}^{(1)} \simeq (0.37 + i 0.60)$ fm^{10,11} are in striking disagreement with the Weinberg-Tomozawa term, the leading order chiral prediction.

The solution to this puzzle lies in the presence of the $\Lambda(1405)$ resonance in the K^- -proton channel^{4,5,14}. The $\Lambda(1405)$ -resonance can be described together with elastic and inelastic K^- -proton scattering data in terms of a coupled channel Lippman-Schwinger equation with the potential matrix evaluated per-

turbatively from the chiral Lagrangian¹⁴. However, the role of chiral symmetry in this approach is unclear. The systematic treatment of important chiral correction terms like range terms or loop effects remains unsettled. Note that a satisfactory description of kaon nucleon scattering data can also be achieved by the coupled K -matrix approach of Martin¹⁰.

As was pointed out first by Koch⁴, the $\Lambda(1405)$ resonance may experience a repulsive mass shift due to Pauli blocking which strongly affects the in-medium K^- -nucleon scattering amplitude^{4,5}. This offers a simple mechanism for the transition from repulsion, implied by the scattering lengths, at low densities, $\rho < 0.1 \rho_0$, to attraction at somewhat larger densities⁵. Schematically this effect can be reproduced in terms of an elementary $\Lambda(1405)$ field dressed by a kaon nucleon loop. The repulsive Λ mass shift due to the Pauli blocking of the nucleon is given by:

$$\Delta m_\Lambda = \frac{g_{\Lambda NK}^2}{\pi^2} \frac{m_N}{m_\Lambda} \left(1 - \frac{\mu_\Lambda}{k_F} \arctan \left(\frac{k_F}{\mu_\Lambda} \right) \right) k_F \quad (4)$$

with the 'small' scale

$$\mu_\Lambda^2 = \frac{m_N}{m_\Lambda} \left(m_K^2 - (m_\Lambda - m_N)^2 \right) \simeq (144 \text{ MeV})^2 \quad (5)$$

and the $\Lambda(1405)$ kaon nucleon coupling constant $g_{\Lambda NK}$.

From (4) we conclude that it is important to extend previous work^{4,6} and treat the K^- -state and the $\Lambda(1405)$ states self consistently¹. We expect self consistency to be important for in-medium K^-N -scattering simply because the characteristic scale μ_Λ in (5) depends sensitively on small variations of m_Λ and m_K . The $\Lambda(1405)$ -resonance mass in matter is now the result of two competing effects: the Pauli blocking increases the mass whereas the decrease of the K^- mass tends to lower the mass.

2 K^- nucleon scattering

We describe K^- nucleon scattering by means of an effective Lagrangian density:

$$\begin{aligned} \mathcal{L} = & \frac{1}{2} g_{11}^{(I=0)} (N^\dagger K) (K^\dagger N) + \frac{1}{\sqrt{6}} g_{12}^{(I=0)} (N^\dagger K) (\vec{\pi}^\dagger \cdot \vec{\Sigma}) \\ & + \frac{1}{\sqrt{6}} g_{21}^{(I=0)} (\vec{\Sigma}^\dagger \cdot \vec{\pi}) (K^\dagger N) + \frac{1}{3} g_{22}^{(I=0)} (\vec{\Sigma}^\dagger \cdot \vec{\pi}) (\vec{\pi}^\dagger \cdot \vec{\Sigma}) \\ & + \frac{1}{2} g_{11}^{(I=1)} (N^\dagger \vec{\tau} K) (K^\dagger \vec{\tau} N) - \frac{1}{2} g_{22}^{(I=1)} (\vec{\Sigma}^\dagger \times \vec{\pi}) (\vec{\pi}^\dagger \times \vec{\Sigma}) \\ & + g_{33}^{(I=1)} (\Lambda^\dagger \vec{\pi}) (\vec{\pi}^\dagger \Lambda) - \frac{i}{2} g_{12}^{(I=1)} \left[(N^\dagger \vec{\tau} K) (\vec{\pi}^\dagger \times \vec{\Sigma}) - h.c. \right] \end{aligned}$$

$$\begin{aligned}
& + \frac{1}{\sqrt{2}} g_{13}^{(I=1)} \left[(N^\dagger \vec{\tau} K) (\vec{\pi}^\dagger \Lambda) + h.c. \right] \\
& - \frac{i}{\sqrt{2}} g_{23}^{(I=1)} \left[(\vec{\Sigma}^\dagger \times \vec{\pi}) (\vec{\pi}^\dagger \Lambda) - h.c. \right]
\end{aligned} \tag{6}$$

with the isospin doublet fields $K = (K_-^\dagger, \bar{K}_0^\dagger)$ and $N = (p, n)$. Here we include the pion, the $\Sigma(1195)$ and the $\Lambda(1115)$ as relevant degrees of freedom since they couple strongly to the K^- -nucleon system. The baryon fields as well as the kaon and pion fields are constructed with relativistic kinematics but without anti-particle components. Technically one represents the interaction strength generated by loops with propagating anti kaons or anti nucleons by local 4-point interaction terms. For the nucleon and kaon this is certainly a 'clean' procedure for energies not far from the kaon nucleon threshold since the kaon and nucleon mass are sufficiently heavy. Integrating out the anti particles of the pion (two-particle irreducible pion loops) is more subtle since one might expect such a scheme to be restricted to energies close to the $\pi\Sigma$ -threshold. Here we assume that the 'small-scale' non-localities which originate from integrating out the anti pions are not important at energies close to the kaon nucleon threshold. Since our scheme describes low energy elastic and inelastic K^- -nucleon scattering data this appears to be justified a posteriori.

The free nucleon and kaon propagator take the form:

$$\begin{aligned}
S_N(\omega, \vec{q}) &= \frac{m_N}{E_N(q)} \frac{1}{\omega - E_N(q) + i\epsilon} \\
S_K(\omega, \vec{q}) &= \frac{1}{2E_K(q)} \frac{1}{\omega - E_K(q) + i\epsilon},
\end{aligned} \tag{7}$$

respectively, where $E_a(q) = \sqrt{m_a^2 + \vec{q}^2}$. The isospin zero coupled channel scattering amplitude

$$T = \begin{pmatrix} T_{KN \rightarrow KN} & T_{KN \rightarrow \pi\Sigma} \\ T_{\pi\Sigma \rightarrow KN} & T_{\pi\Sigma \rightarrow \pi\Sigma} \end{pmatrix} \tag{8}$$

is given by the set of ladder diagrams conveniently resummed in terms of the Bethe-Salpeter integral equation. Since the interaction terms in (6) are local the Bethe-Salpeter equation reduces to the simple matrix equation

$$T(s) = g(s) + g(s) J(s) T(s) = (g^{-1}(s) - J(s))^{-1}. \tag{9}$$

with the loop matrix $J = \text{diag } (J_{KN}, J_{\pi\Sigma})$ and

$$\begin{aligned}
J_{KN}(\omega, \vec{q}) &= - \int_0^\lambda \frac{d^3 l}{(2\pi)^3} \frac{m_N}{E_N(l)} S_K(\omega - E_N(l), \vec{q} - \vec{l}) \\
J_{\pi\Sigma}(\omega, \vec{q}) &= - \int_0^\lambda \frac{d^3 l}{(2\pi)^3} \frac{m_\Sigma}{E_\Sigma(l)} S_\pi(\omega - E_\Sigma(l), \vec{q} - \vec{l}).
\end{aligned} \tag{10}$$

Small range terms are included in our scheme by the replacements $g_{11} \rightarrow g_{11} + h_{11}(s - (m_N + m_K)^2)$, $g_{12} \rightarrow g_{12} + h_{12}(s - (m_N + m_K)^2)$ and $g_{22} \rightarrow g_{22} + h_{22}(s - (m_\Sigma + m_\pi)^2)$ induced by appropriate additional terms in (6). The loop functions J_{KN} and $J_{\pi\Sigma}$ are regularized by the cutoff $\lambda = 0.7$ GeV.

We construct the $I = 1$ coupled channel scattering amplitude in full analogy to the isospin zero case with $J = \text{diag}(J_{KN}, J_{\pi\Sigma}, J_{\pi\Lambda})$ (see eq. (9)). The range terms are included by the replacements $g_{11} \rightarrow g_{11} + h_{11}(s - (m_N + m_K)^2)$, $g_{12} \rightarrow g_{12} + h_{12}(s - (m_N + m_K)^2)$, $g_{13} \rightarrow g_{13} + h_{13}(s - (m_N + m_K)^2)$, $g_{22} \rightarrow g_{22} + h_{22}(s - (m_\Sigma + m_\pi)^2)$ and $g_{33} \rightarrow g_{33} + h_{33}(s - (m_\Lambda + m_\pi)^2)$.

The Lagrangian density (6) follows from a chiral Lagrangian with relativistic baryon and meson fields upon integrating out the anti-particle field components. Therefore the coupling matrix g is constrained to some extent by chiral symmetry¹⁴. To leading order one may derive the isospin zero coupling strengths by matching tree level threshold amplitudes. The chiral matching of correction terms and the range parameters h_{ij} is less obvious. In fact a consistent chiral matching requires the K^- -nucleon potential to be evaluated minimally at chiral order Q^3 . Only at this order the necessary counter terms for the loop functions are introduced. Recall that, as was emphasized by Kolck¹⁵, only the cutoff dependent real part of the loop functions trigger the desired sign change of the K^- proton scattering length.

In this work the coupling strengths g_{ij} are directly adjusted to reproduce empirical scattering data described in terms of the coupled channel scattering amplitude (9). Here we might loose some constraint from chiral symmetry. The effective range parameters h_{ij} , on the other hand, we construct according to the $SU(3)$ -symmetry of the chiral Lagrangian since they are not affected by the chiral Q^3 counter terms. This implies that the range terms in the isospin one channel can be expressed in terms of the isospin zero range parameters and one free parameter h_F

$$\begin{aligned}
h_{11}^{(I=1)} &= \frac{1}{2} \left(h_{11}^{(I=0)} - \sqrt{6} h_{12}^{(I=0)} + h_{22}^{(I=0)} - 6 h_F \right) \\
h_{12}^{(I=1)} &= \frac{1}{6} \left(3 h_{11}^{(I=0)} + \sqrt{6} h_{12}^{(I=0)} - 3 h_{22}^{(I=0)} - 6 h_F \right) \\
h_{13}^{(I=1)} &= \frac{1}{12\sqrt{6}} \left(6 h_{11}^{(I=0)} + 2\sqrt{6} h_{12}^{(I=0)} - 6 h_{22}^{(I=0)} + 36 h_F \right) \\
h_{22}^{(I=1)} &= \frac{1}{12} \left(15 h_{11}^{(I=0)} - 5\sqrt{6} h_{12}^{(I=0)} - 3 h_{22}^{(I=0)} - 30 h_F \right) \\
h_{23}^{(I=1)} &= 0 \\
h_{33}^{(I=1)} &= \frac{1}{9} \left(3 h_{11}^{(I=0)} - 5\sqrt{6} h_{12}^{(I=0)} + 6 h_{22}^{(I=0)} - 18 h_F \right)
\end{aligned} \tag{11}$$

The imposed $SU(3)$ -symmetry for the range parameters (11) is an important

ingredient for our subthreshold extrapolation of the K^-N -scattering amplitude in the $I = 1$ channel. Note that the chiral approach of reference ¹⁴ starts with a SU(3) symmetric interaction. However, the use of different cutoff values in the various loop integrals obscures the SU(3)-symmetry constraint.

In the isospin zero channel the set of parameters $g_{11}\lambda = 46.86$, $g_{12}\lambda = 11.67$, $g_{22}\lambda = 16.08$, $h_{11}\lambda^3 = 0.79$, $h_{12}\lambda^3 = 8.57$ and $h_{22}\lambda^3 = 4.94$ follows from a least square fit to the amplitudes of ¹⁴. The isospin one amplitudes $K^-N \rightarrow K^-N, \pi\Sigma, \pi\Lambda$ of ¹⁴ are described well with $g_{23} = g_{33} = 0$ as suggested by the leading order Weinberg Tomozawa term and $g_{11}\lambda = 12.75$, $g_{12}\lambda = 13.56$, $g_{13}\lambda = 15.07$, $g_{22}\lambda = 16.04$ and $h_F\lambda^3 = -1.92$.

We obtain a good description of all coupled channel amplitudes with the scattering lengths $a_{K^-N}^{(I=0)} \simeq (-1.76 + i 0.60)$ fm and $a_{K^-N}^{(I=1)} \simeq (0.35 + i 0.69)$ fm close to the values obtained by Martin ¹⁰.

3 K^- in nuclear matter

The kaon self energy $\Pi_K(\omega, \vec{q})$ is evaluated in the nucleon gas approximation

$$\Pi_K(\omega, \vec{q}) = -4 \int_0^{k_F} \frac{d^3 l}{(2\pi)^3} \frac{m_N}{E_N(l)} \bar{T}_{KN}(\omega + E_N(l), \vec{q} + \vec{l}) \quad (12)$$

in terms of the in medium kaon nucleon scattering amplitude $4\bar{T}_{KN} = \bar{T}_{KN}^{(I=0)} + 3\bar{T}_{KN}^{(I=1)}$. The scattering amplitude \bar{T}_{KN} is given by (9) with the vacuum kaon nucleon loop J_{KN} replaced by the in matter loop \bar{J}_{KN} with

$$\bar{J}_{KN}(\omega, \vec{q}) = - \int_{k_F}^{\lambda} \frac{d^3 l}{(2\pi)^3} \frac{m_N}{E_N(l)} \bar{S}_K(\omega - E_N(l), \vec{q} - \vec{l}) \quad (13)$$

and the Fermi momentum k_F . The in medium kaon nucleon loop, $\bar{J}_{KN}(\omega, \vec{q})$ is regularized by our cutoff parameter λ such as to reproduce the vacuum loop function $J_{KN}(\omega, \vec{q})$ in the zero density limit. Selfconsistency is met once \bar{J}_{KN} is evaluated in terms of the kaon propagator:

$$\bar{S}_K(\omega, \vec{q}) = \frac{1}{2E_K(q)} \frac{1}{\omega - E_K(q) - \Pi_K(\omega, \vec{q})/(2E_K(q)) + i\epsilon} \quad (14)$$

with the kaon self energy $\Pi_K(\omega, \vec{q})$ of (12).

In Fig. 2 we present our final self-consistent result for the kaon spectral density as a function of the kaon energy ω for various Fermi momenta k_F and kaon momenta \vec{q} . Typically the spectral density exhibits a two peak structure representing the K^- and the $\Lambda(1405)$ -nucleon hole states. As the Fermi

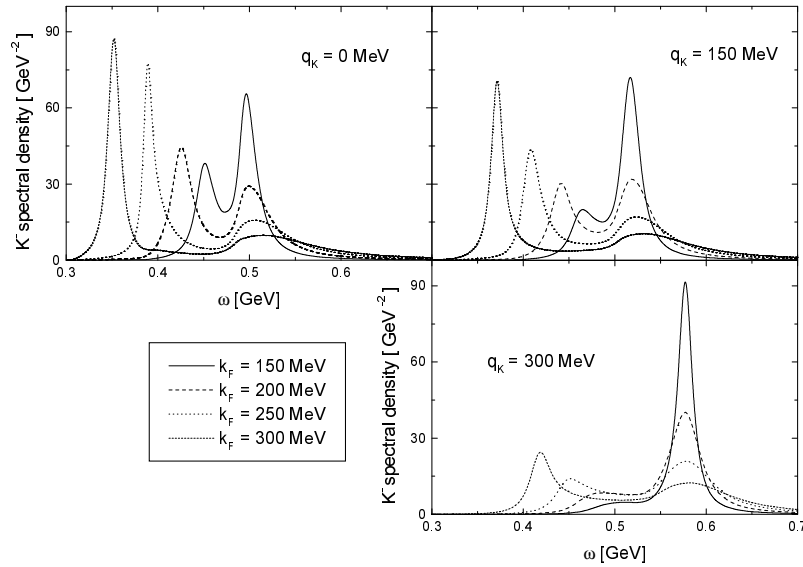


Figure 2: K^- spectral density for kaon momenta $q_K = 0$, $q_K = 150$ MeV and $q_K = 300$ MeV in isospin symmetric nuclear matter. The spectral density is evaluated self consistently with respect to the propagation of the $\Lambda(1405)$ resonance.

momentum k_F increases the energetically lower state experiences a strong attractive shift whereas the more massive state becomes broader. On the other hand as the kaon momentum increases both states basically gain kinetic energy with the energetically higher peak attaining more strength.

It is instructive to compare various approximations for the kaon self energy: the kaon self energy as evaluated i) with the Pauli blocked kaon nucleon scattering amplitude (the approximation scheme applied in ^{4,5,6}), ii) with the self consistent amplitude and iii) with the free space amplitude. All three schemes predict a two mode structure of the kaon spectral density, however, with quantitative differences. Both, the Pauli blocked and the self-consistent amplitude shift strength from the upper branch to the lower branch as compared with the spectral density derived from the free space amplitude. While the Pauli blocked amplitude causes a small repulsive shift of the $\Lambda(1405)$ -nucleon-hole state the self-consistent amplitude predicts an attractive shift. At larger densities self consistency affects the K^- -rest mass moderately. For example at $k_F = 300$ MeV we find $\Delta m_{K^-} \simeq -140$ MeV and $\Gamma_{K^-} \simeq 35$

MeV as compared with $\Delta m_{K^-} \simeq -141$ MeV and $\Gamma_{K^-} \simeq 31$ MeV from the free space amplitude and $\Delta m_{K^-} \simeq -123$ MeV and $\Gamma_{K^-} \simeq 29$ MeV from the Pauli-blocked amplitude. Note here that the quasi particle width $\Gamma_{K^-} = -\Im \Pi(m_{K^-} + \Delta m_{K^-}, \vec{q} = 0)/(m_{K^-} + \Delta m_{K^-})$, given above, differs from the physical K^- -width by about a factor of two due to the strong energy dependence of the kaon self energy (see Fig. 2). We find that self consistency is most important once the K^- -mode starts moving relative to the nuclear medium. Here we expect p-wave K^-N -interactions¹⁷, which are not included in this work, to modify our results to some extent.

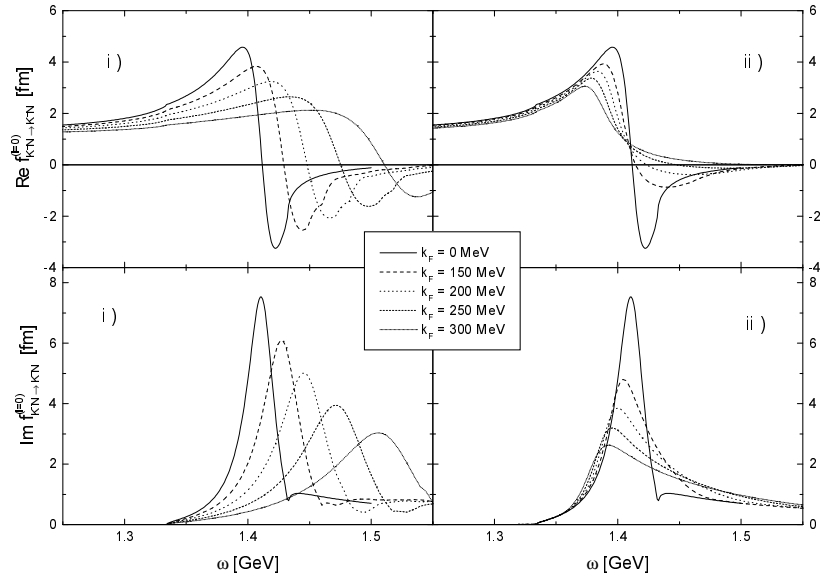


Figure 3: Isospin zero elastic K^- -nucleon scattering amplitude in nuclear matter evaluated i) with Pauli blocked kaon nucleon loop and ii) with self-consistent loop. Here $q_N + q_K = 0$.

We turn to in medium K^- nucleon scattering. Fig. 3 shows the isospin zero elastic scattering amplitude

$$f_{K^-N \rightarrow K^-N}^{(I=0)}(\omega, \vec{q}) = \frac{m_N}{4\pi\omega} T_{K^-N \rightarrow K^-N}^{(I=0)}(\omega, \vec{q}) \quad (15)$$

evaluated with i) the Pauli blocked kaon nucleon loop and ii) the self-consistent kaon nucleon loop at $|\vec{q}_K + \vec{q}_N| = 0$. The two amplitudes differ dramatically as the Fermi momentum is increased. In the Pauli-blocked amplitude i) the

$\Lambda(1405)$ resonance peak is shifted to higher energies whereas the self consistent amplitude ii) predicts the resonance peak to remain more or less at its free space position. Note that the $\Lambda(1405)$ mass shift of the Pauli-blocked amplitude can be reproduced rather accurately with eq. (4) and $g_{\Lambda NK} \simeq 2.3$. We conclude that the attractive feedback effect of a decreased kaon mass, as included in the self-consistent approach, is important for the structure of the $\Lambda(1405)$ resonance in nuclear matter. Altogether the $\Lambda(1405)$ resonance mass is basically unchanged, however, the resonance acquires an increased decay width as nuclear matter is compressed. Furthermore we point out that the real part of the elastic scattering amplitude is strongly modified: it changes its sign for $\omega > m_N + m_K$ from repulsion to attraction as the density gets larger.

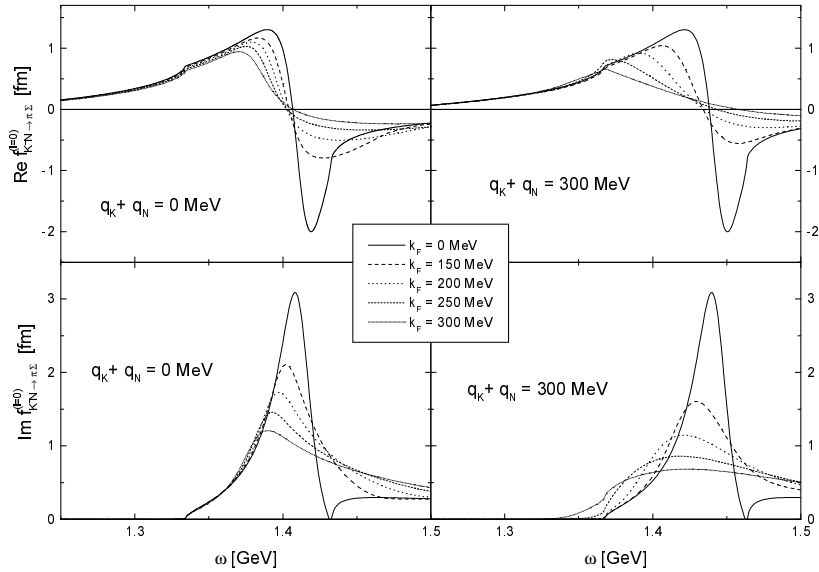


Figure 4: Isospin zero $\pi\Sigma$ production amplitude in nuclear matter evaluated with self-consistent kaon nucleon loop.

We turn to the inelastic channels. Fig. 4 shows the isospin zero $\pi\Sigma$ production amplitude

$$f_{K^- N \rightarrow \pi\Sigma}^{(I=0)}(\omega, \vec{q}) = \frac{\sqrt{m_N m_\Sigma}}{4\pi\omega} T_{K^- N \rightarrow \pi\Sigma}^{(I=0)}(\omega, \vec{q}) \quad (16)$$

evaluated with the self-consistent kaon nucleon loop at $|\vec{q}_K + \vec{q}_N| = 0$ and

$|\vec{q}_K + \vec{q}_N| = 300$ MeV. The imaginary part of the amplitude shows a clear peak around 1.4 GeV for all Fermi momenta representing the $\Lambda(1405)$ resonance state. This confirms the structure of the resonance as seen in the elastic channel at $|\vec{q}_K + \vec{q}_N| = 0$ MeV. On the other hand, at the larger momentum $|\vec{q}_K + \vec{q}_N| = 300$ MeV the resonance broadens more quickly and disappears at large Fermi momenta.

We point out that the production amplitude, $f_{K-N \rightarrow \pi\Sigma}^{(I=0)}$, is changed considerably close to the kaon nucleon threshold. Finally in Fig. 5 and Fig. 6 we

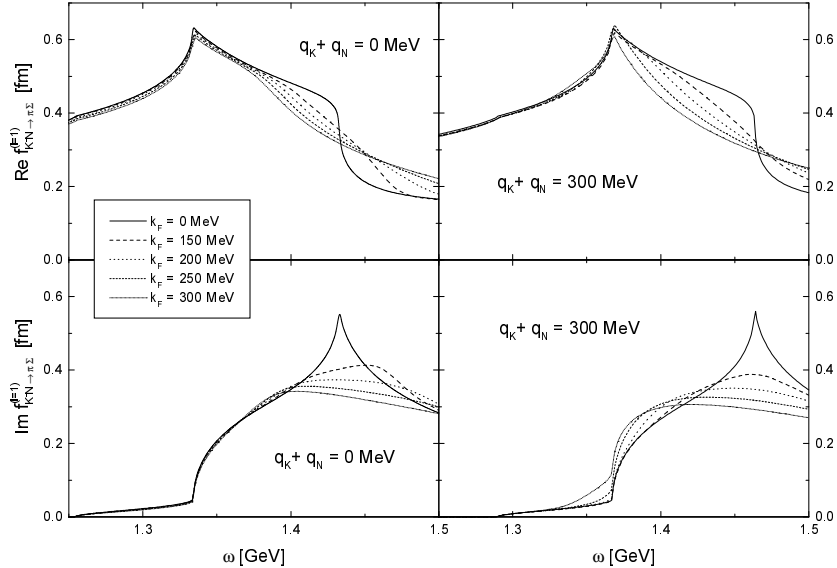


Figure 5: Isospin one $\pi\Sigma$ production amplitude in nuclear matter evaluated with self-consistent kaon nucleon loop.

present our result for the isospin one $\pi\Sigma$ and $\pi\Lambda$ production amplitudes. Again the kaon nucleon threshold region of the amplitudes is affected strongly. We conclude that the $\pi\Sigma$ and $\pi\Lambda$ production branching ratios are modified strongly in nuclear matter. This should have important consequences for pion and kaon production in heavy ion collision at energies where the production spectra are sensitive to the detailed dynamics of low energy kaon nucleon scattering¹⁸.

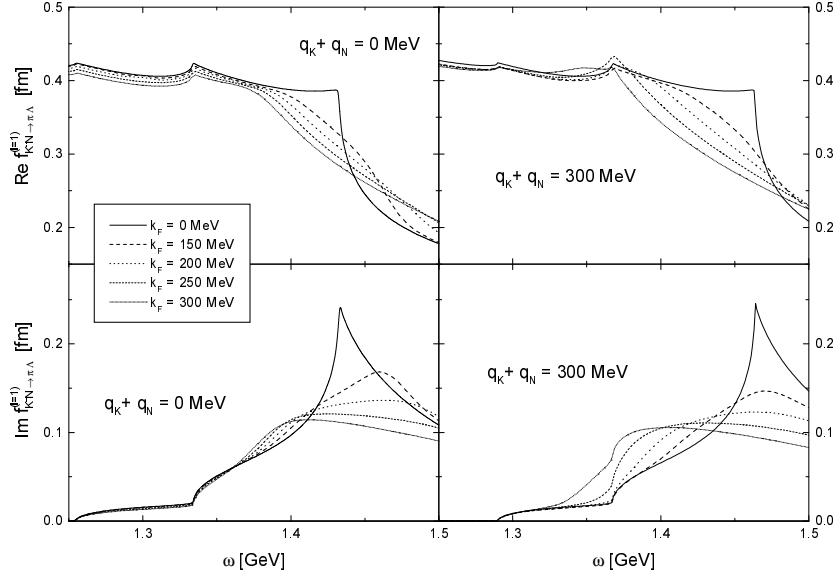


Figure 6: Isospin one $\pi\Lambda$ production amplitude in nuclear matter evaluated with self-consistent kaon nucleon loop.

4 K^- -nuclear optical potential

Kaonic atom data provide a valuable consistency check on any microscopic theory of K^- nucleon interaction in nuclear matter. For a recent review see ¹³. It is therefore important to apply our microscopic approach also to kaonic atoms.

K^- atoms are described in terms of the Klein Gordon equation

$$\left[\vec{\nabla} \cdot \vec{\nabla} - \mu^2 + \left(\omega - V_c(r) \right)^2 - 2\mu U_{opt}(\vec{r}, \vec{\nabla}) \right] \phi(\vec{r}) = 0 \quad (17)$$

with the Coulomb potential $V_c(r)$ of the finite nucleus including the proper vacuum polarization and $U_{opt}(\vec{r}, \vec{\nabla})$ the K^- nuclear optical potential. Here μ is the reduced mass of the kaon nucleus system. The binding energy E and decay width Γ of the kaonic atom state follow with $\omega = \mu + E - i\Gamma/2$.

The optical potential $U_{opt}(\vec{r}, \vec{\nabla})$ is related to the K^- self energy in nuclear matter. In the extreme low density limit the optical potential is determined

by the s-wave K^-N scattering length:

$$2\mu U_{opt}(\vec{r}, \vec{\nabla}) = -4\pi \left(1 + \frac{m_K}{m_N}\right) a_{K^-N} \rho(r) \quad (18)$$

with

$$a_{K^-N} = \frac{1}{4} \left(a_{K^-N}^{(I=0)} + 3 a_{K^-N}^{(I=1)} \right) \simeq (-0.18 + 0.67i) \text{ fm} \quad (19)$$

and the nucleus density profile $\rho(r)$. The optical potential (18) does not describe kaonic atoms well. Friedman et al. show that kaonic atom data can be described with a large attractive effective scattering length $a_{eff} \simeq (0.63 + 0.89i)$ fm which is in direct contradiction with the low density optical potential (18).

We compare this large attractive scattering length of Friedman et al. with the density dependent effective scattering length

$$\Pi_{K^-}(\omega = m_K, \vec{q} = 0) = -\frac{8}{3\pi} \left(1 + \frac{m_K}{m_N}\right) a_{eff}(k_F) k_F^3. \quad (20)$$

predicted by our kaon self energy $\Sigma_{K^-}(\omega, \vec{q}^2)$. The real part of the effective scattering length $a_{eff}(k_F)$, shown in Fig. 7, changes sign as the density is increased. At large densities we find an attractive scattering length. This is a welcome effect. However as shown in ¹⁹ this effect falls short in explaining kaonic atom data. A good description of data requires a large attractive effective scattering length at $k_F < 150$ MeV if non-local interaction terms were small. We conclude that the explanation of kaonic atoms with a density dependent effective scattering length but with only small gradient interaction terms is ruled out by our microscopic approach.

We proceed and discuss non-local effects. Mizoguchi et al. ²⁰ use a optical potential of the form

$$2\mu U_{opt}(\vec{r}, \vec{\nabla}) = -4\pi \left(1 + \frac{m_K}{m_N}\right) \left(a_{K^-N} \rho(r) - b \vec{\nabla} \rho(r) \cdot \vec{\nabla} \right) \quad (21)$$

with the phenomenological parameter $b \simeq (0.47 + i 0.30)$ fm³ adjusted to reproduce kaonic atom data.

It is instructive to confront the phenomenological parameter b with our microscopic approach. We extract an effective slope parameter, $b_{eff}(k_F)$,

$$\begin{aligned} \Pi_{K^-}(\omega = m_K, \vec{q}) &= -\frac{8}{3\pi} \left(1 + \frac{m_K}{m_N}\right) a_{eff}(k_F) k_F^3 \\ &\quad - \frac{8}{3\pi} \left(1 + \frac{m_K}{m_N}\right) b_{eff}(k_F) k_F^2 \vec{q}^2 + \mathcal{O}(\vec{q}^4) \end{aligned} \quad (22)$$

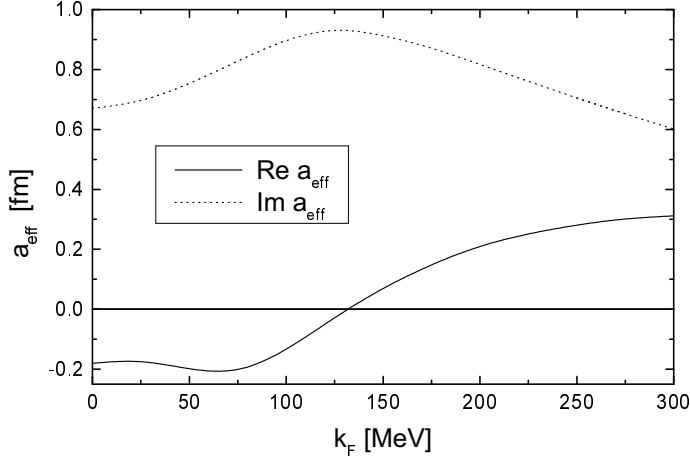


Figure 7: The effective scattering length $a_{eff}(k_F)$ defined in eq. (20).

from our self energy with $|\vec{q}| < k_F$. Naively one may identify $k_F b = b_{eff}(k_F)$. We point out that the effective slope parameter, shown in Fig. 8, changes sign at the rather small Fermi momentum $k_F \simeq 75$ MeV. At larger densities our microscopic approach predicts attractive non-local interaction strength of considerable size. At a typical Fermi momentum $k_F = 150$ MeV we find

$$b \leftrightarrow \frac{1}{k_F} b_{eff}(k_F) \simeq (0.13 + i 0.13) \text{ fm}^3 \quad \text{at} \quad k_F = 150 \text{ MeV} \quad (23)$$

a value smaller than the result of Mizoguchi et al.. Together with the attraction from our effective scattering length and a small residual attractive p-wave interaction term we expect a good description of kaonic atom data.

We point out that the form of the non-local interaction as implied by our microscopic approach differs from the phenomenological potential of Mizoguchi et al.. The s-wave K^- -nucleon interaction implies the following form of the optical potential:

$$\begin{aligned} 2\mu U_{opt}(\vec{r}, \vec{\nabla}) &= -4\pi \left(1 + \frac{m_K}{m_N}\right) a_{eff}(k_F(r)) \rho(r) \\ &+ \frac{8}{3\pi} \left(1 + \frac{m_K}{m_N}\right) \left(1 + \frac{m_K}{2m_N}\right) \vec{\nabla} k_F^2(r) b_{eff}(k_F(r)) \vec{\nabla} \end{aligned}$$

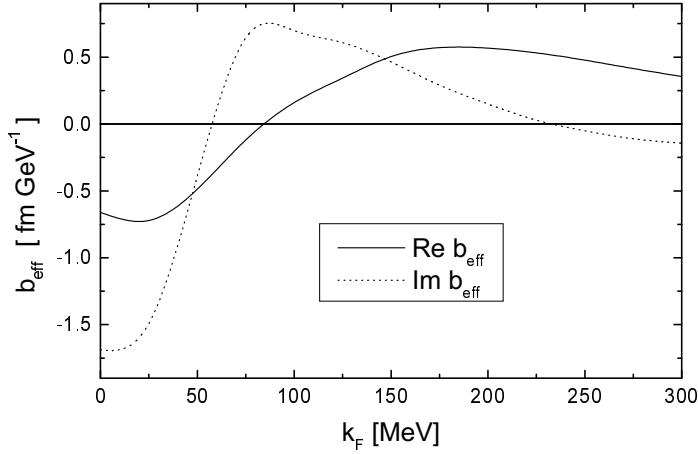


Figure 8: The effective slope parameter $b_{eff}(k_F)$ defined in eq. (22).

$$- \frac{8}{3\pi} \left(1 + \frac{m_K}{m_N}\right) \frac{m_K}{4m_N} \left[\vec{\nabla}^2, k_F^2(r) b_{eff}(k_F(r)) \right]_+ \quad (24)$$

with the ordering of the gradients derived in ¹⁹. Our optical potential (24) together with a small attractive p-wave interaction term (induced by the $Y(1385)$ resonance in the K^-n channel) is confronted with kaonic atom data in ¹⁹.

Acknowledgments

The author is grateful for useful discussions with W. Florkowski, B. Friman, E. Kolomeitsev and D.-P. Min.

References

1. M. Lutz, nucl-th/9709073
2. G.E. Brown and M. Rho, *Nucl. Phys. A* **596**, 503 (1996); G.Q. Li, C.-H.Lee, G.E. Brown, nucl-th/9706057.
3. H. Yabu et al. *Phys. Lett. B* **315**, 17 (1993).
4. V. Koch, *Phys. Lett. B* **337**, 7 (1994).

5. T. Waas, N. Kaiser and W. Weise, *Phys. Lett. B* **365**, 12 (1996), *Phys. Lett. B* **379**, 34 (1996).
6. T. Waas, M. Rho and W. Weise, *Nucl. Phys. A* **617**, 449 (1997).
7. V.R. Pandharipande, C.J. Pethick and V. Thorsson, *Phys. Rev. Lett.* **75**, 4567 (1995).
8. C.-H. Lee, D.-P. Min and M. Rho, *Nucl. Phys. A* **602**, 334 (1996).
9. M. Lutz, A. Steiner and W. Weise, *Nucl. Phys. A* **574**, 755 (1994).
10. A.D. Martin, *Nucl. Phys. A* **179**, 33 (1981).
11. M. Iwasaki et al., *Phys. Rev. Lett.* **78**, 3067 (1997).
12. E. Friedman, A. Gal and C.J. Batty, *Nucl. Phys. A* **579**, 518 (1994).
13. C.J. Batty, E. Friedman and A. Gal, *Phys. Rep.* **287**, 385 (1997)
14. N. Kaiser, P.B. Siegel and W. Weise, *Nucl. Phys. A* **594**, 325 (1995); N. Kaiser, T. Waas and W. Weise, *Nucl. Phys. A* **612**, 297 (1997); T. Waas, private communication.
15. U. van Kolck, private communication
16. C.L. Korpa and R. Malfliet, *Phys. Rev. C* **52**, 2756 (1995)
17. E.E. Kolomeitsev, D.N. Voskresensky, B. Kämpfer, *Nucl. Phys. A* **588**, 889 (1995).
18. C. B. Dover, D.J. Millener and A. Gal, *Phys. Rep.* **184**, 1 (1989); A.S. Rosenthal and F. Tabakin, *Phys. Rev. C* **22**, 711 (1980); A. Ohnishi, Y. Nara and V. Koch, nucl-th/9706084
19. W. Florkowski and M.F.M. Lutz, in preparation
20. M. Mizoguchi, S. Hirenzaki and H. Toki, *Nucl. Phys. A* **567**, 893 (1994)